JOURNAL OF MATERIALS SCIENCE 26 (1991) 5107–5112

Chemical and structural characterization of SnS_2 single crystals grown by low-temperature chemical vapour transport

T. SHIBATA*, Y. MURANUSHI, T. MIURA, T. KISHI
Department of Applied Chemistry, Faculty of Science and Technology, Keio University, Hiyoshi 3-14-1, Kouhoku-ku, Yokohama 223, Japan

Chemical and structural characterization has been performed for thick (100–600 μm) and thin (10–100 μm) 2H/4H inter-polytype SnS_2 crystals grown by low-temperature chemical vapour transport in the reverse temperature gradient geometry. X-ray diffraction shows that the 2H/4H-SnS_2 phase transforms to single-crystal 2H-SnS_2 in 6–12 months. The S/Sn ratio is 2.02 ± 0.01 in thick crystals and 2.01 ± 0.01 in thin crystals. Thermogravimetric/differential thermal analysis and the other characterization techniques show no difference between the two types of crystal. Extremely small quantities of carbon and oxygen and some chlorine were detected by secondary ion mass spectroscopy and/or X-ray photoelectron spectroscopy (XPS). These elements are concentrated at the surface. The XPS data show a chemical shift of tin and sulphur in the surface layer, which is probably caused by the adsorbed carbon and oxygen; however, it cannot be explained by the formation of the usual oxides of tin and sulphur.

1. Introduction

Single crystals of the semiconducting group IV chalcogenide SnS_2 have been grown by the novel low-temperature chemical vapour transport method developed by the authors [1]. Powdered SnS_2 is used as the charge material and $SnCl_4 \cdot 5H_2O$ as the transport agent. The method employs a reverse temperature gradient, with the transport zone kept at 419–438 °C and the growth zone at 449–455 °C. These temperatures are around 200 °C lower than those employed previously [2]. The single crystals grown by our method are platelets up to 10 mm × 35 mm side dimensions, that can be divided into two categories: crystals (100–600 μm thick), which are orange in colour, and crystals (10–100 μm thick), which are yellow. In the remainder of this paper, these crystals will be designated as thick or thin, respectively. Some growth runs yield a small number of thick platelets, some runs many thin platelets only. In some runs a few thick ones of small volume coexisting with many thin ones are obtained. A significant difference other than thickness is that some of the thick platelets have a hexagonal growth pattern, which is not found in thin ones.

Because the physical properties of semiconductors are generally influenced by small amounts of impurities or variations in the synthesis method, thorough characterization is necessary to understand these properties. Nevertheless there are few reports on the characterization of synthesized SnS_2. Furthermore, the existence of inter-polytypes [3, 4] complicates interpretation of the results. This paper presents chemical and structural characterization results for SnS_2 single crystals grown by the low-temperature vapour transport method.

Polytype determination was performed by X-ray and electron diffraction. The S/Sn ratio was found by thermogravimetric analysis. The thermal behaviour in air was examined by thermogravimetric/differential thermal analysis (TG/DTA), impurities were identified and depth-profiled by secondary ion mass spectrometry (SIMS), and the binding energies of surface and bulk elements were measured by X-ray photoemission spectroscopy (XPS).

2. Experimental procedure

2.1. Composition analysis

The z values of two samples of SnS_z were calculated from the weight change (Mettler, AE240) that occurred when the samples were oxidized on heating in an electric furnace (Motoyama, Super Burn) in air from room temperature to 1200 °C at a rate of 20 °C min^{-1}, held at 1200 °C for 6 h, and finally cooled gradually back to room temperature. One sample consisted of 247.90 mg thick crystals, the other of 162.80 mg thin crystals. They were placed in separate alumina crucibles, which had been brought to constant weight by being fired three times at 1400 °C for 6 h each. The oxide was identified as SnO_2 by X-ray diffraction (XRD). The samples were examined for residual sulphur by electron probe microanalysis (EPMA) (Shimadzu, EMX-SM). SnO_2 powder (Mitsuwa, 99.99% pure) was used as a standard to correct for volatilization during heating.

*Present address: Department of Biochemistry, Tokyo Women's Medical College, Kawada-cho 8-1 Shinjuku-ku, Tokyo 162, Japan.

0022–2461/91 $03.00 + .12 © 1991 Chapman & Hall

2.2. Thermal analysis

TG/DTA (Rigaku TG/DTA 8078G2 on-line with Thermal Analysis Station TAS100) was performed on 20 mg samples of 1 mm^2 crystal platelets in platinum pans that were heated in air from room temperature to 1400 °C at a rate of 10 °C min^{-1}. Powdered Al_2O_3 was used as the DTA standard.

2.3. Crystal structure

Transmission electron diffraction (Jeol, JEM-8T) was performed on a cleaved specimen that was mounted with glue on a meshgrid. Debye rings of a vacuum-deposited gold thin film were used as a standard diffraction pattern.

X-ray diffraction analysis (Rigaku, RADIIA) was performed at room temperature by scanning the range $3° < 2\theta < 140°$ at rates of 1/16–2° min^{-1}. The CuK_{α_1} line (0.154 06 nm), a graphite monochromator, and power of 40 kV, 20 mA were used. Samples were attached with an adhesive compound to an aluminium sample holder. Powdered silicon was used as a standard.

2.4. SIMS analysis of impurities

SIMS (Cameca, SIMS 3F) was performed using O_2^+ (10.5 keV, 1.0 µA) as the primary ion for positive ion analysis over the mass range 1–120 AMU, and Cs^+ (14.5 keV, 0.2 µA) as the primary ion for negative ion analysis over the mass range 1–60 AMU. The primary ion was raster scanned over an area of 250 × 250 μm^2, and the diameter of the detection area of the secondary ions was 60 µm. The cleaved surface of a single crystal was used for all measurements.

2.5. Analysis by XPS

Measurements of binding energy were carried out by XPS (Jeol, JPS-90SX), using MgK_α X-rays at an energy of 10 kV and current of 20 mA. The single-crystal sample was fixed to a sample holder with silver paste (Tokuriki, P-246). Each sample was cleaved in air immediately before measurement to expose an (0 0 1) face. Sampling time was 20–50 ms for each 0.05 eV scanning step and ten-time accumulation was made. The pressure was 5×10^{-6} Pa or less. For depth profiling, etching was performed at a pressure of 2×10^{-2} Pa with an argon ion current of 8 mA at an accelerating voltage of 500 V. The etching rate was about 0.4 nm min^{-1} [5].

Binding energies of Sn $3d_{5/2}$, Sn $4d_{5/2,3/2}$, S $2p_{3/2,1/2}$, C $1s_{1/2}$, and O $1s_{1/2}$ were measured for six samples and found to be reproducible. Correction of binding energy was made with respect to C $1s_{1/2}$ energy at 285.0 eV on the sample surface.

Curve smoothing of an observed spectrum was performed using nine neighbouring points. The peak value was taken to be the centre of gravity of the integrated intensity after background subtraction. Shape analysis was performed based on mixed distribution of Lorentzian and Gaussian fitting.

3. Results and discussion

3.1. Composition analysis

The values of z measured for the SnS_z samples composed of thick and thin crystals are 2.02 ± 0.01 and 2.01 ± 0.01, respectively. For both samples, the densities measured with a pycnometer under reduced pressure were less than 4.5 g cm^{-3}, the X-ray density calculated from the lattice parameters [6]. These results indicate that both types of crystal have lattice vacancies at tin sites.

The value of z in SnS_z has usually been reported to be less than or equal to 2. Our samples may be sulphur-rich because of the relatively low temperature used in our crystal growth technique.

The sulphur-rich SnS_2 material should have p-type conductivity; however, contrary to this prediction, these materials showed n-type semiconductivity on investigation of the electrical characterization [7]. SnS_2 is generally known as n-type from almost all reports [8].

3.2. Thermal analysis

Fig. 1 shows weight loss with an exothermic reaction beginning near 450 °C, which corresponds to thermal decomposition of SnS_2 following oxidation, finally

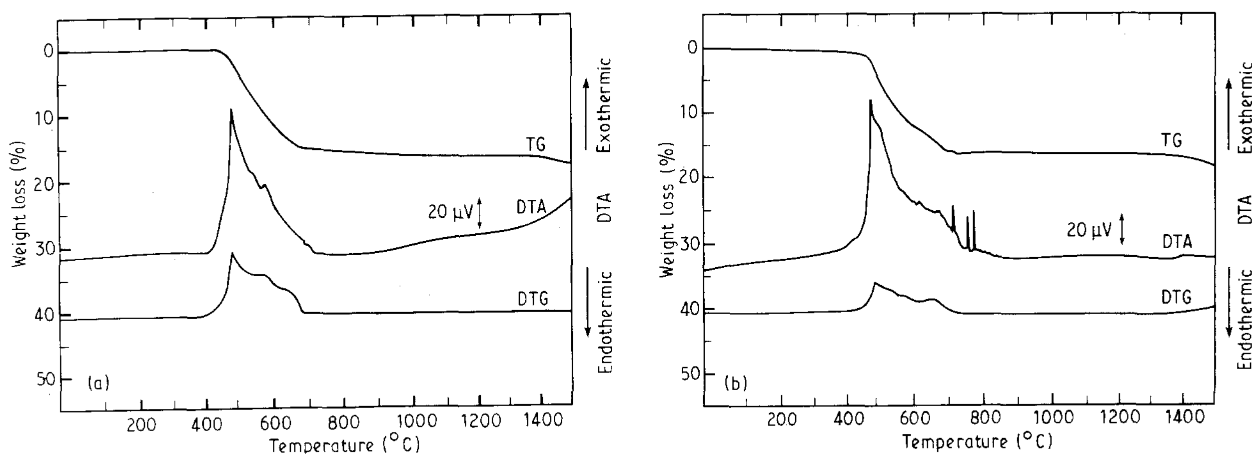

Figure 1 TG, DTA and DTG results for (a) thick and (b) thin SnS_2 crystals.

being oxidized to SnO_2. The three sharp exothermic peaks observed at 700–800 °C for the thin SnS_2 sample are probably not caused by the phase transition of a polytype, but by the reaction of some sulphur that had been enclosed by an oxide layer. (As discussed in the following section, XRD indicates the presence of 2H and less stable 4H stacking in both thick and thin samples, but the fraction of 4H is probably too low for its transition to 2H to be detected by DTA.) Except for these exothermic peaks, there is no significant difference between the results for the thick and thin samples.

3.3. Crystal structure

In almost all sampled areas, the electron diffractogram shows a hexagonal pattern, as shown in Fig. 2a, with an a-plane lattice constant $a = 0.36$ nm. In addition, the possibility of a superlattice structure within the c-plane is suggested, because some sampled areas show a superlattice-like pattern in which satellite diffractions are observed around the main reflections, as shown in Fig. 2b. The origin of the satellite spots has not been identified.

The $(00l)$ XRD data are listed for both thick and thin samples in Table I. There are two types of $(00l)$ peaks. One series of peaks, starting at $2\theta = 15.01°$, corresponds to 2H-SnS_2. Lattice constants are refined to be $a = 0.3647(1)$ and $c = 0.5899(1)$ nm (hexagonal, $P\bar{3}m1$) using all XRD data of stress-free powder samples of SnS_2. On the other hand, a diffraction peak corresponding to the (001) Bragg reflection of 4H-SnS_2 is observed at $2\theta = 7.487°$, as shown in Fig. 3. The peak intensity is around 0.2% of the strongest (001) peak of 2H-type at $2\theta = 15.01°$. Both thick and thin crystals are, therefore, identified as 2H/4H inter-polytypes [3, 4] that contain a small fraction of the 4H-SnS_2 stacking sequence in 2H-SnS_2.

The (001) peak of 4H-SnS_2 was no longer observed after a sample had been kept in air at room temperature for several months or a year. This implies that 2H-SnS_2 is more stable than 4H-SnS_2. A similar phenomenon is observed when the intercalation reaction of the cations by the electrochemical method is performed for a 2H/4H inter-polytype host material. The 4H structure is gradually transformed into the 2H structure, as will be reported elsewhere.

3.4. SIMS analysis of impurities

No impurities were detected by positive ion analysis, while molecules or ions containing carbon, oxygen

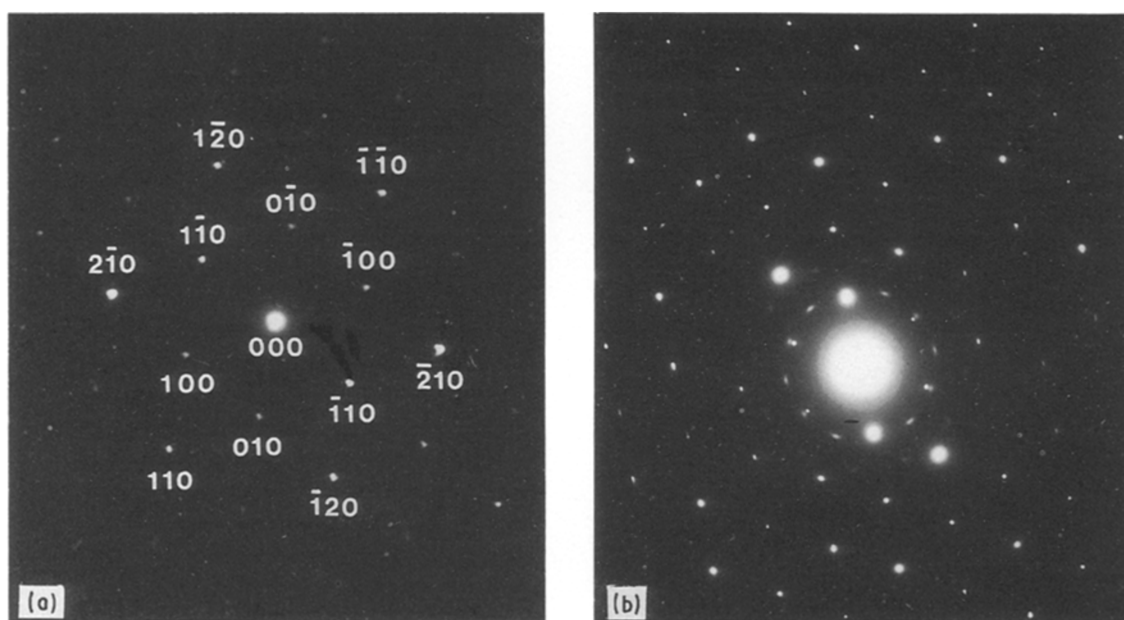

Figure 2 Electron diffraction patterns within a c-plane obtained from (a) 2H-SnS_2 and (b) a sampled area showing satellite diffraction.

TABLE I $(00l)$ XRD patterns for thick and thin samples

$(h\,k\,l)$		Thick sample			Thin sample		
2H-type	4H-type	d(nm)	I_o	FWHM (deg)	d(nm)	I_o	FWHM (deg)
	001	1.1793	0.25	0.25	1.1798	0.13	0.25
001	002	0.5897	100.00	0.12	0.5899	100.00	0.10
002	004	0.2948	11.32	0.15	0.2950	12.46	0.11
003	006	0.1966	18.36	0.15	0.1966	20.89	0.09
004	008	0.1474	18.36	0.14	0.1475	18.53	0.09
005	0010	0.1179	13.61	0.13	0.1180	6.04	0.09
006	0012	0.0983	2.36	0.10	0.0983	0.79	0.09
007	0014	0.0842	0.23	0.14	0.0843	2.55	0.15

and chlorine were detected in some regions of a thick sample by negative ion analysis. Impurities having mass number over 64 cannot be measured, because of the detection limit.

Although a mass spectrum was difficult according to a measurement point by the influence of contamination from the surface, no significant difference was observed between thick and thin crystals. Fig. 4 shows typical depth profiles for tin, carbon, oxygen and chlorine of both thick and thin crystals. Carbon, oxygen and chlorine were detected at the same depth within a thin single crystal.

No elements other than tin and sulphur were detected in depth profile measurements using Augar electron spectroscopy. This discrepancy is due to the difference in the probe areas. Therefore, it is suggested that carbon, oxygen and chlorine are confined in the crystals in a localized manner.

3.5. XPS analysis

Depth profiles of XPS spectra are represented in Table II and Fig. 5. No differences in binding energies were observed between thick and thin samples.

The XPS data show that carbon and oxygen are adsorbed on the surface of the SnS_2 crystals. The concentrations of carbon and oxygen in the bulk are only about 1/15 and 1/40, respectively, of the surface concentrations. A C $1s_{1/2}$ peak at 289.25 eV was observed at the surface for a few samples. The O $1s_{1/2}$ peak at 532.68 eV is believed to correspond mainly to double bonds of oxygen, because this binding energy is a little larger than the value of 532 eV for elemental oxygen [9]. The large FWHM indicates the presence of various bonding states. A chemical shift was observed between surface oxygen and bulk oxygen.

The binding energy of Sn $3d_{5/2}$ is 486.40 eV in the bulk, in agreement with the reported value of 486.6 eV [10]. This orbital shows a chemical shift by 1 eV to higher energy near the surface. The value at the surface is much larger than the binding energy of 486.4 eV in SnO [11] and SnO_2 [12]. The cause of the shift has not been determined. A similar chemical shift is observed for other tin and sulphur orbitals.

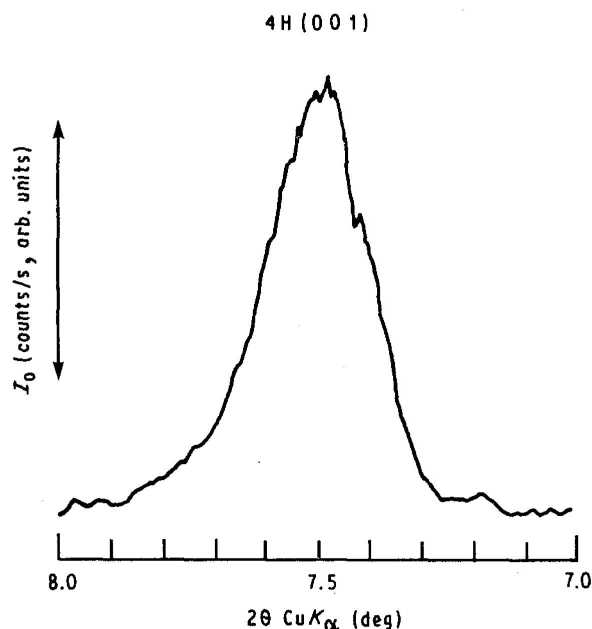

Figure 3 Rocking curve corresponding to (001) XRD of 4H-SnS_2.

TABLE II XPS binding energies of single-crystal SnS_2 on the surface and in the bulk

	Binding energy (eV)	
	Surface	Bulk
S $2s_{1/2}$	226.78 (2.40)	
S 2p	162.37 (2.04)	161.37 (2.21)
S $2p_{3/2}$	162.25 (1.30)	161.60 (1.30)
$2p_{1/2}$	163.40 (1.40)	162.82 (1.40)
Sn $3p_{3/2}$	717.10 (3.66)	
$3p_{1/2}$	759.15 (3.53)	
Sn $3d_{5/2}$	487.47 (1.67)	486.40 (1.82)
$3d_{3/2}$	495.90 (1.62)	
Sn 4d	26.50 (2.17)	25.68 (2.35)
Sn $4d_{5/2}$	26.25 (1.20)	25.15 (1.20)
$4d_{3/2}$	27.35 (1.30)	26.22 (1.30)
C $1s_{1/2}$	285.00 (2.30)	284.75 (2.12)
	289.25 (1.28)	—
O $1s_{1/2}$	532.68 (2.75)	530.87 (2.68)

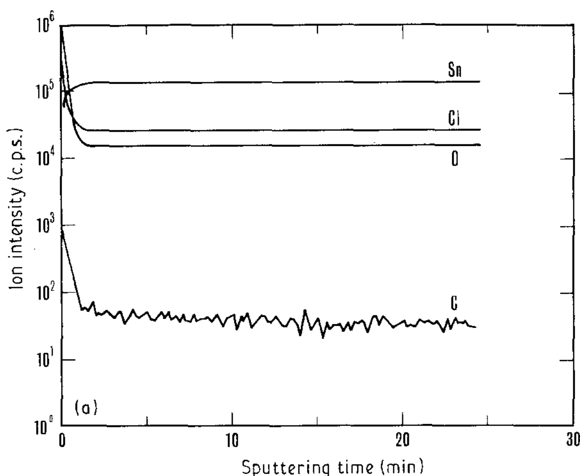

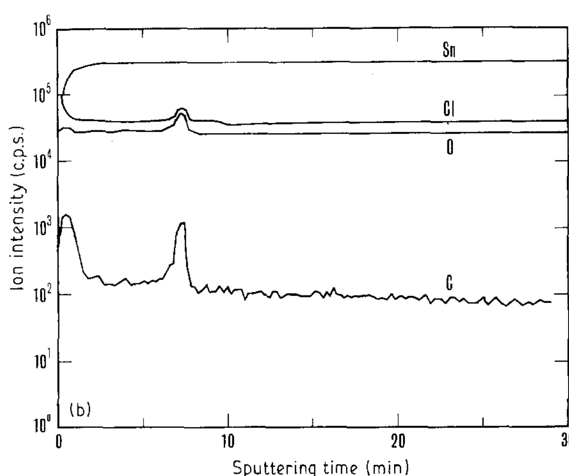

Figure 4 SIMS depth profiles for tin, carbon, oxygen and chlorine in (a) thick and (b) thin crystals.

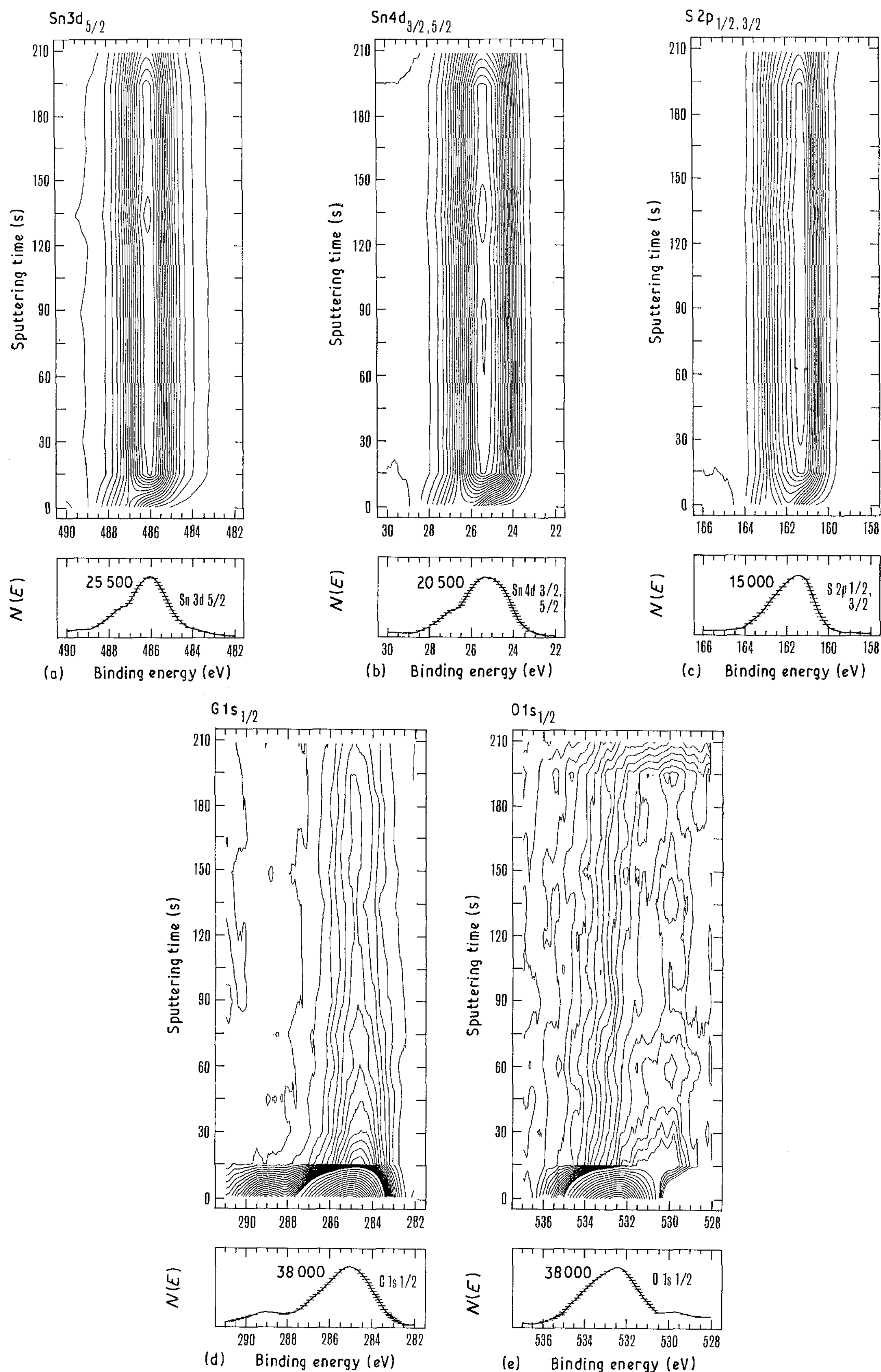

Figure 5 XPS maps (depth profile) of single-crystal SnS_2. The lower plots are projection charts showing the relation between binding energy and signal intensity $N(E)$ counts/s. Horizontal bars show intervals of contour lines. (a) Sn $3d_{5/2}$, (b) Sn $4d_{5/2,3/2}$, (c) S $2p_{3/2,1/2}$, (d) C $1s_{1/2}$, (e) 0 $1s_{1/2}$.

4. Conclusion

Chemical and structural characterization results have been presented for 2H/4H inter-polytype thick (100–600 μm) and thin (10–100 μm) crystals of SnS_2. XRD showed that the 2H/4H-SnS_2 transforms to 2H-SnS_2 over a period of several months to a year at room temperature. Composition analysis gave unusual sulphur-rich values, $z = 2.01 \pm 0.01$ in thin crystals and $z = 2.02 \pm 0.01$ in thick ones. Small concentrations of carbon, oxygen and chlorine in the bulk of the crystals were detected by SIMS measurements. We believe that carbon and oxygen were incorporated from these

adsorbed on the surface of the SnS_2 powder used as the starting material, while chlorine was introduced by the transport agent. XPS measurements also showed the presence of carbon and oxygen adsorbed on the surface of SnS_2 single crystals. Chemical shifts of the orbitals of tin and sulphur were observed, which cannot be explained by the formation of the usual oxides of tin and sulphur. The advantages of the low-temperature chemical vapour transport method are that a larger volume of single-crystals can be obtained than by the high-temperature chemical vapour transport method, and that pure 2H-SnS_2 single phase crystals can be obtained after transition, differently from the mixture of many polytypes by the high-temperature methods. It is difficult to compare our 2H-SnS_2 single crystals with others obtained by high temperature using iodine as a transport agent, because few papers concerned with the chemical characterization are available.

Acknowledgements
The authors thank Dr N. Kambe, NTT Basic Research Laboratories, for SIMS, Assistant Professor Dr E. Ohta, Keio University, for lending electron diffraction equipment, Assistant Professor Dr H. Hirashima for lending TG/DTA equipment, and Professor Dr S. Anzai for helpful discussion of superlattices.

References
1. T. SHIBATA, T. MIURA, T. KISHI and T. NAGAI, *J. Crystal Growth*, **106** (1990) 593.
2. F. A. S. AL-ALAMY and A. A. BALCHIN, *ibid.* **38** (1977) 221.
3. B. PALOSZ, W. PALOSZ and S. GIERLOTAKA, *Bull. Mineral.* **109** (1986) 143.
4. *Idem, Acta Crystallogr.* **C41** (1985) 807.
5. T. SHIBATA, Y. MURANUSHI, T. MIURA and T. KISHI, *Hyomen Gijutsu* **40** (1989) 1142.
6. F. J. SCHMITTE, in Landolt Bornstein, "Group III: Crystal and Solid State Physics, Semiconductors", Vol. 17d, edited by K. H. Hellwege and O. Madelung (Springer-Verlag, Berlin, 1983) p. 207.
7. T. SHIBATA, Y. MURANUSHI, T. MIURA and T. KISHI, *J. Phys. Chem. Solids*, **52** (1991) 551.
8. G. DOMINGO, R. S. ITOGA and C, R. KANNEWURF, *Phys. Rev.* **143** (1965) 536.
9. S. HAGSTROM and S. E. KARLSSON, *Arkiv Fysik* **26** (1964) 451.
10. W. E. MORGAN and J. R. VAN WAZER, *J. Phys. Chem.* **77** (1973) 96.
11. P. A. GRUTSCH, M. V. ZELLER and T. P. FEHLNER, *Inorg. Chem.* **12** (1973) 1432.
12. A. W. C. LIN, N. R. ARMSTRONG and T. KUWANA, *Anal. Chem.* **49** (1977) 1228.

Received 17 August 1990
and accepted 24 January 1991